Desalination and Water Treatment
www.deswater.com

doi: 10.1080/19443994.2014.883577

54 (2015) 382–392
April

Taylor & Francis
Taylor & Francis Group

Phenol photodegradation process assisted with Wells–Dawson heteropolyacids

Adel Balaska[a,b,*], Mohamed ElHadi Samar[b], Azzeddine Grid[c]

[a]*Laboratory of Environmental Engineering, Faculty of Engineering, Department of Process Engineering, Badji Mokhtar-Annaba University, P.O. Box 12, Annaba 23000, Algeria*
Tel./Fax: +21 338876560; email: balaskaa@yahoo.fr
[b]*National Welding and Control Research Center, Iron and Steel Applied Research Unit (U.R.A.S.M/C.S.C), P.O. Box 196, Annaba 23000, Algeria*
[c]*National Welding and Control Research Center, Industrial Technologies Research Unit (U.R.T.I/C.S.C), P.O. Box 1037, Annaba 23000, Algeria*

Received 23 June 2013; Accepted 10 January 2014

ABSTRACT

This work aims to investigate the catalytic properties of the heteropolyacids (HPAs) within photocatalytic process. Photocatalytic degradation of phenol in aqueous solution was performed using Wells–Dawson HPAs as catalysts under UV-illuminated condition at 254 nm. The effects of various parameters such as, concentration of catalyst, initial pH, and initial phenol concentration on the performance of photocatalytic process have been investigated to obtain the efficient and durable catalysts and determine the better reaction conditions. The kinetics and the efficiency of phenol degradation were determined by various analytical techniques, such as HPLC and TOC. The results show that the photocatalytic degradation efficiency increases with decreasing pH and the optimum pH is 2 for both catalysts. The photodegradation follows pseudo-first-order kinetics with rate constants $k = 8.56 \times 10^{-2}$ and $9.94 \times 10^{-2}\,\text{min}^{-1}$ for iron- and vanadium-substituted HPAs, respectively.

Keywords: Wells–Dawson HPA; Homogeneous catalysis; Phenol photodegradation; UV irradiation

1. Introduction

Nowadays, the pollution of water resources becomes a very serious problem attracting more and more concerns. Among all kinds of contaminants, phenol, widely used as an industrial raw material or intermediate, is one of the most toxic organic discharged by numerous manufactories [1]. Phenol gives an unpleasant taste and odor to drinking water and can exert negative effects on different biological processes. In the presence of chlorine, phenol forms chlorophenols [2] which are readily absorbed by gastrointestinal tract causing acute toxicity and increase respiratory rate followed by vomiting and nausea. Even for concentrations as low as 0.1 mg/L, chlorophenols produce an objectionable taste when they are mixed with drinking water [3]. The toxicity increases with the degree of chlorination which could generate mutagenic and carcinogenic chlorophenols

---

*Corresponding author.

compounds. Therefore, increasingly stringent restrictions have been imposed on the concentrations of phenol in drinking water and in wastewater for safe discharge [2]. Biological degradation, membrane filtration, ion exchange, reverse osmosis, adsorption, biosorption, oxidation with hydrogen peroxide, wet oxidation, electrochemical oxidation, and photocatalytic degradation have been used for the removal of phenols [3]. The most conventional processes have significant disadvantages such as incomplete ion removal, high-energy requirements, production of toxic sludge, or other waste products that require further disposal. The efficiency and simplicity of advanced oxidation processes (AOPs) make them a suitable choice for the removal of toxic chemicals from wastewater in the recent years [4–6]. AOPs are very promising, well known for their oxidizing efficiency even in traces. Especially, titanium dioxide (TiO_2) and polyoxometalates (POMs) photocatalysis are more elegant and practical [7].

In general, POMs constitute a large category of well-defined metal oxygen cluster anions, formed by condensation of mainly tungstates and/or molybdates with or without participation of a variety of other elements [8–10]. Together with the Keggin anion, the Wells−Dawson molecule is probably the second heteropolyanion in popularity. POMs Dawson type [11] is formed by the connection of metal-oxygen polyhedral building blocks via covalent bonding. The central metal atoms are usually tungsten and/or molybdenum [12]. Acidification of the tungstate and the molybdate solutions in the presence of other anions leads to the incorporation of these anions at the center of the polyanion to form the so-called heteropolyanions or POMs [13]. Wells−Dawson heteropolyanion structure can be formulated as $[(X^{n+})_2M_{18}O_{62}]^{(16-2n)-}$ or $[(X^{n+})_2M_{15}M_3{}'O_{62}]^{(16-2n)-}$, where X^{n+} represents a central atom (heteroatom) such as P and Si, surrounded by a cage of M or M′ addenda atoms, such as Mo^{6+} or W^{6+} or a mixture of elements. Recently, the use of heteropoly compounds as catalysts in both homogeneous and heterogeneous processes has attracted great interest in organic synthesis because their stronger Brönsted acidity, their redox properties can be controlled at the molecular or atomic level and they also offer economical and environmental benefits [14], where the majority of POMs are not toxic and inexpensive [15]. Yamase [16], Song and Barteau [17] and Hiskia et al. [18] have used the POMs as photocatalysts in many catalytic reactions and they proved that the POMs are well-organized metal-oxygen cluster anion, which initiates a variety of redox reactions under UV-illuminated condition [19]. Hiskia et al. [18], Bae et al. [19] and Kim et al. [20] have also demonstrated that the features and photo-behavior of POMs are similar to those of semiconductor metal oxides and have a wide application as catalysts. Troupis et al. [7], have examined the photocatalytic reductive degradation of azo dye by four POMs: $PW_{12}O_{40}^{3-}$, $SiW_{12}O_{40}^{4-}$, $P_2W_{18}O_{62}^{6-}$, and $P_2Mo_{18}O_{62}^{6-}$ in order to examine the influence of the kind of POM on the process efficiency. They have shown that by taking advantage of POMs ability to exhibit widely, yet precisely varied redox potentials (Table 1). The redox control is imposed in the process of degradation, where a rapid photocatalytic reduction decoloration is obtained by a series of polyoxotungstates POMs in the presence of a sacrificial reagent propan-2-ol following the order $PW_{12}O_{40}^{3-} > SiW_{12}O_{40}^{4-} > P_2W_{18}O_{62}^{6-}$ and no effect of polyoxomolybdates.

Heteropolyacid (HPA) is the tertiary structure of POM. Catalysis by HPAs is a field of increasing importance, in which many new and exciting developments are taking place in both research and technology [21]. HPAs possess unique properties such as: well-defined structure, ability to accept and release electrons, high proton mobility, and possibility to modify their acid–base and redox properties by changing their chemical composition [22,23]. In addition to their stronger Brönsted acidity, one of the great advantages of HPAs catalysts is that their catalytic properties can be tuned in a systematic way by replacing protons or by substituting framework transition metal atoms with different metals [24].

The present paper covers the synthesis of several Wells–Dawson HPAs, followed by application of these HPAs in homogeneous photocatalytic process i.e. using vanadium-substituted HPA (V-HPA) and iron-substituted HPA-Dawson type as photocatalysts for phenol degradation in aqueous solution. The efficiency of photocatalytic process is evaluated by examining, initial phenol concentration, pH, and catalysts loading. The effects of operational key parameters on phenol photodegradation under ambient conditions are obtained and the first-order rate kinetics is evaluated.

2. Materials and methods

2.1. Catalysts preparation

In 1953, Dawson was the first who characterized and determined the position of the heteroatom by single X-ray crystal study. The synthesis of potassium salt $\alpha/\beta\text{-}K_6P_2W_{18}O_{62}$ is the central of most works based primarily on Wells–Dawson type heteropolyanions [10,25–27]. In this work, the diphosphooctadecatungstic salt $\alpha_1K_6P_2W_{18}O_{62}.14H_2O$, the unsubstituted HPA $H_6P_2W_{18}O_{62}.14H_2O$, V-HPA

Table 1
Reduction potentials of the POMs photocatalysts [7]

POM	$P_2W_{18}O_{62}{}^{6-/8-}$	$P_2W_{18}O_{62}{}^{6-/7-}$	$PW_{12}O_{40}{}^{3-/4-}$	$SiW_{12}O_{40}{}^{4-/5-}$
Potentials E°(volts)	+0.664	+0.334	+0.221	+0.057

$H_7P_2W_{17}VO_{62}.14H_2O$, the molybdo-tungsto-diphosphates salt α-$K_6P_2W_{12}Mo_5{\cdot}10H_2O$, the unsubstituted HPA $H_6P_2W_{12}Mo_5{\cdot}10H_2O$, and iron-containing HPA (Fe-HPA) $H_5P_2W_{12}Mo_5Fe{\cdot}10H_2O$ were prepared according to the methods reported in the literature [8,28–34].

All solvents and reagents for synthesis were purchased from Aldrich at least grade of purity. Phenol and other chemicals including, H_2SO_4, NaOH, and acetonitrile were all offered from Merck as analytical reagent grade. All catalysts were recrystallized twice, dried in a vacuum, and kept at room temperature in desiccators.

2.2. Analytical methods

Photodegradation of phenol was monitored by HPLC using Merck-Hitachi HPLC apparatus equipped with UV/vis detector (L-4250. 190–700 nm) and a pump (model L-6200) and a 5 μm C_{18} reversed-phase column (250 mm × 4.6 mm ID). Acetonitrile/water mobile phase was 70/30 and the flow rate was 1 mL/min. Aliquots of 20 μL were injected onto a reversed phase and analyzed by UV/vis detector at 254 nm wavelength.

The progress of the total mineralization of phenol during the treatment was monitored by measuring dissolved organic carbon using a liquid TOC II analyzer. Reproducible TOC values were obtained from analysis of variable sample volumes between 0.04 and 4 mL and fast multipoint calibration with one standard solution. During all experiments, samples were immediately measured without using any filter. Moreover, the pH solution was adjusted at desired value by adding concentrated sulfuric acid (H_2SO_4.98%) or sodium hydroxide solution (NaOH, 0.1 M). Then, the pH and temperature were measured using a digital pH-T-meter (Hanna Instruments, model HI 8424 N).

2.3. Photodegradation experiments

Photocatalytic activity of the synthesized catalysts was evaluated using aqueous solution of phenol under ultraviolet irradiation. All degradation experiments were conducted in a Pyrex cylindrical photoreactor with 0.85 L capacity. A UV lamp (high-pressure mercury lamp Heraeus, TQ 718 of 700 W), emitting at 254 nm wavelength, was positioned at the center of the cylindrical vessel and surrounded by circulating water jacket to keep room temperature (25 ± 1°C) during the reactions. The reactor is covered with an aluminum sheet so that no stray light can enter to the reactor and to prevent loss of UV light. The stirring was accomplished by means of a closed circulating loop using a pump at a flow rate of 150 L/h. The flow system was assembled with poly-tetra-fluor-ethylene tubing and connectors. The schematic diagram of the experimental setup used in this study is shown in Fig. 1.

Decomposition and mineralization of phenol in the presence or absence of HPAs have been studied. The degradation efficiency of phenol is defined as follows:

$$\text{Degradation efficiency} = \frac{C_0 - C}{C_0} \times 100 \tag{1}$$

where C_0 is the initial concentration of phenol and C is the phenol concentration at photolysis time (t).

Moreover, the degradation efficiency is evaluated using the kinetics models to represent the influence of catalysts loading. The Langmuir–Hinshelwood model is usually used to describe the kinetics of photocatalytic reactions of aquatic organics [35–37]. In most photocatalytic kinetic studies, it is assumed that the low concentration used in the experiments allowed that the model can be simplified to the first-order kinetics which is expressed by the following equation:

$$\ln\left(\frac{C}{C_0}\right) = -kt \tag{2}$$

A plotting of $-\ln(C/C_0)$ vs. illumination time (t) yields a straight line, where the slope is the rate constant k. The photodegradation and the rate reaction depend on several factors. To study the effect of these variables, the experiments were repeated under different pH values (1.9–4), catalyst concentrations (6–14 mM), and initial phenol concentrations (0.32–1.27 mM). The experiments were performed for 120 min and the liquid samples were taken at preset time intervals.

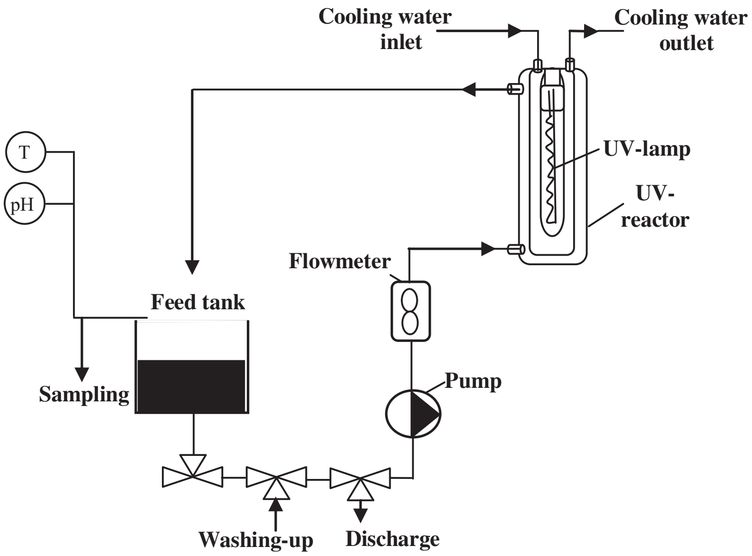

Fig. 1. Schematic diagram of the photocatalytic degradation reactor setup.

3. Results and discussion

3.1. Effect of UV irradiation and photocatalyst containing phenol

The photodegradability of phenol has been investigated by exposing the phenol solutions to UV light only and in the presence of 8 mM of catalyst.

Fig. 2 shows the photodegradation of 1.06 mM phenol in aqueous solutions under various reaction conditions. The results demonstrate that the efficiency of degradation increases with the UV-irradiation exposure time. The phenol photodegradation is not significant in the absence of catalyst where the degradation of phenol is less than 35% within 60 min in the direct photolysis. Moreover, in the presence of V-HPA and Fe-HPA catalysts, almost 96 and 89% of phenol have been degraded within 60 min, respectively.

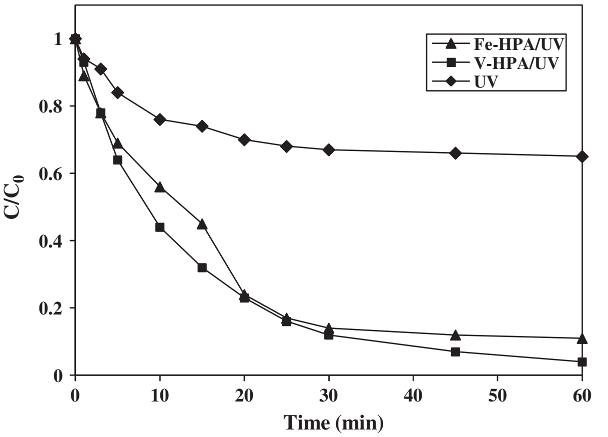

Fig. 2. Photodegradation of phenol by direct photolysis and by HPA/UV processes. Experimental conditions: $[C_0] = 1.06$ mM, [HPA] = 8 mM, $t = 60$ min, pH = 2.5, and $T = 25$°C.

3.2. Effect of initial phenol concentration

The effect of initial concentrations of phenol on the degradation has been investigated between 0.32 and 1.27 mM of phenol solutions. The photodegradation by Fe-HPA/UV and V-HPA/UV are shown in Figs. 3 and 4, respectively.

It is observed that the degradation efficiency increases with the decreasing initial concentration using 8 mM of both catalysts. When $C_0 < 0.32$ mM, 100% of phenol is degraded only within 45 min of irradiation in the presence of V-HPA and within 60 min in the presence of Fe-HPA. Under the same conditions stated above, C_0 increases up to 1.27 mM, 79 and 74% of phenol are removed, respectively. At $C_0 = 1.27$ mM, the degradation efficiency does not exceed 88% within 120 min of irradiation using Fe-HPA catalyst and 100% of phenol is degraded within only 105 min using V-HPA catalyst.

The calculated values of the initial rate (r_{in}) are used to confirm previous results. At the beginning of irradiation, degradation rate is expressed by the initial degradation rate as follows:

$$r_{in} = kC_0 \tag{3}$$

The results of initial photocatalytic degradation rates are given in Table 2.

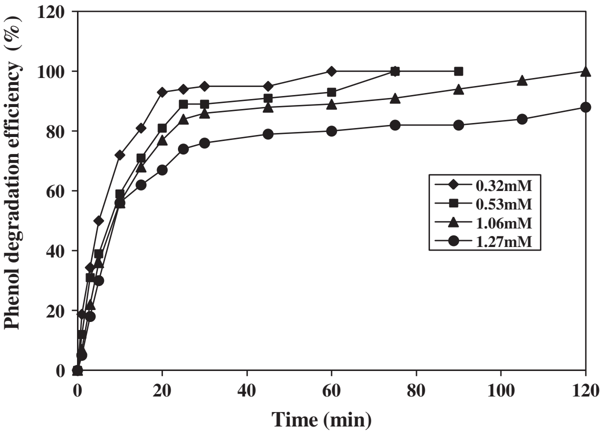

Fig. 3. Effect of the initial phenol concentration on photodegradation. Experimental conditions: [Fe-HPA] = 8 mM, $t = 120$ min, pH = 2.5 and $T = 25$°C.

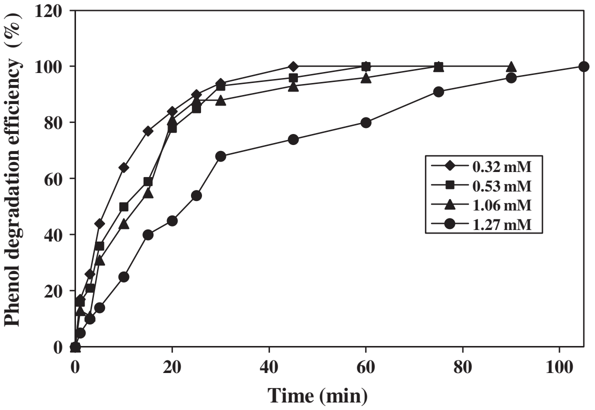

Fig. 4. Effect of the initial phenol concentration on photodegradation. Experimental conditions: [V-HPA] = 8mM, $t = 120$ min, pH = 2.5 and $T = 25$°C.

As shown in Table 2, the initial rate increases with the initial phenol concentration from 0.32 to 1.06 mM, but r_{in} decreases when the initial concentration exceeds 1.06 mM. The increasing of phenol concentration is beneficial to allow more phenol molecules to react with the hydroxyl radicals. However, too high phenol concentration could be unfavorable to the UV light penetration because the yellow color of phenol solution becomes more and more dark and then becomes impermeable to UV irradiation which decreases the initial rate.

Many researchers proved that the initial rate of photocatalytic reactions is a function of other parameters. Chin [38] reported that the photocatalytic initial reaction rate is a function of initial species concentration (C_0), catalyst weight/concentration (C_C), and rate of photon absorption (P_a) (Eq. (4)). He indicated that when C_C increases, the initial reaction rate increases until a maximum is achieved, corresponding to the total absorption of incident light. No benefit is observed from further increasing of C_C because the additional catalyst does not participate in the photoreaction.

$$r_{in} = f(C_0)f(C_C)f(P_a) \tag{4}$$

Therefore, the degradation rate (k) and the photodegradation efficiency decrease vs. the initial phenol concentration i.e. increase of initial concentration decelerates the rate of degradation and the amount of catalyst is not sufficient for the degradation.

The present results are consistent with previous works [7,39] and indicate that the photocatalytic degradation process using HPA/UV is rather promising at lower reactant concentrations. From previous tests, we can initially conclude that V-HPA is the most promising catalyst for phenol photodegradation.

3.3. Effect of pH

pH is an important parameter in photodegradation because the photocatalysis takes place on the surface of photocatalyst and the pH determines the surface charge of the photocatalysts.

Moreover, pH plays an important role in the stability of HPAs in aqueous solution, because the majority of HPAs, namely the Wells–Dawson type are only stable in acidic environment [40]. In this work, the effect of pH value has been studied in a range 1.9–4 because the Wells–Dawson HPAs are only stable at pH < 4 [23]. Fig. 5 shows the effect of pH on the photocatalytic degradation of phenol.

The results show a significant effect of pH. In general, the degradation efficiency of phenol increases with decreasing pH.

It is seen that in a pH range (1.9–2.5): a complete degradation of phenol by V-HPA/UV process is achieved and about 90% of phenol has been degraded by Fe-HPA/UV process, where the pH 2 is more favorable for both HPAs.

To clarify the mechanism of re-oxidation of the reduced HPA(e$^-$) by O_2 in solution, below are given redox reactions involved in the reduction of dioxygen in an acidic aqueous solution with the corresponding redox potentials. These data allow to set a thermodynamic assessment to explain how the re-oxidation of HPA(e$^-$) takes place.

Table 2
Initial degradation rates of phenol solutions

C_0 (mM)	Fe-HPA		V-HPA	
	k (min^{-1})	r_{in} (mM min^{-1})	k (min^{-1})	r_{in} (mM min^{-1})
0.32	0.1187	0.0380	0.1319	0.0422
0.53	0.0848	0.0449	0.1004	0.0532
1.06	0.0760	0.0808	0.0817	0.0868
1.27	0.0623	0.0791	0.067	0.0851

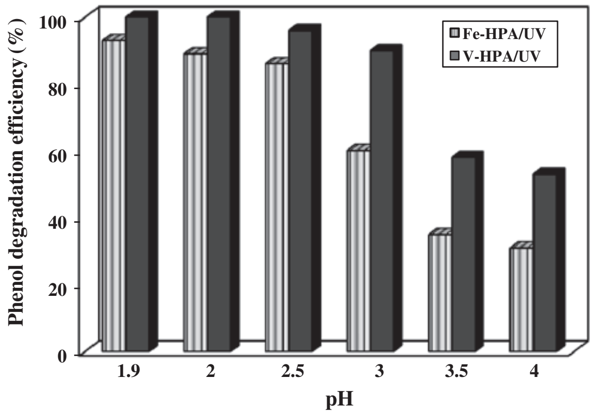

Fig. 5. Effect of pH on phenol photodegradation in different processes. Experimental conditions: $[C_0] = 1.06$ mM $[\text{HPA}] = 8$ mM, $t = 60$ min, and $T = 25$°C.

$$O_2 + e^- + H^+ \rightarrow HO_2^{\bullet} \quad E = -0.05V \tag{5}$$

$$O_2 + 2e^- + 2H^+ \rightarrow H_2O_2 \quad E = 0.68V \tag{6}$$

$$O_2 + 4e^- + 4H^+ \rightarrow 2H_2O \quad E = 1.23V \tag{7}$$

Efforts have been made by Park et al. [24,41] to determine the relationship between reduction potential of HPA and their catalytic activity. They have obtained that the HPAs which have high reduction potentials showed high oxidation yields.

It can be seen from Eq. (5) that O_2 is a rather poor one electron oxidant and the oxidation of the reduced HPA(e^-) with O_2 to form $HO_2^{\bullet}$ radical is highly unfavorable thermodynamically (low potential). However, two or four electron oxidations are feasible (Eqs. (6) and (7)). Consequently, the reduced HPA(e^-) is more re-oxidized with high electron oxidation number and high proton H^+ number i.e. pH should be decreased [42].

3.4. Effect of catalyst concentration

The concentration of catalyst is an important operating parameter to be investigated to insure the total absorption of efficient photons without undesirable excess of catalyst.

The influence of HPA loading on the rate of phenol degradation has been investigated within 20 min, while keeping the same experimental conditions ($C_0 = 1.06$ mM, pH = 2, and $T = 25$°C). The effect of catalysts loading is presented in Figs. 6 and 7 and the pseudo-first-order rate constants of reaction at different loading are shown in the following table:

The results presented in Figs. 6 and 7 show that the photodegradation efficiency increases with the catalyst concentration from 6 to 14 mM. With reference to k values in Table 3, it is found that the linear relationship is consistent. It is also observed that, the degradation efficiency increases as a function of catalyst concentration, following the order $6 < 8 < 10 < 12 < 14$. Furthermore, the photodegradation of phenol is best and fastest at the following catalysts optimal concentrations: [Fe-HPA] = 12 mM and [V-HPA] = 10 mM, where their rate constants values are found $k = 8.56 \times 10^{-2}$ and 9.94×10^{-2} min^{-1}, respectively. According to these results, it has been decided to keep HPAs concentrations at the optimum value in subsequent photocatalytic degradation experiments. Beyond the optimum dose, the photodegradation is constant and

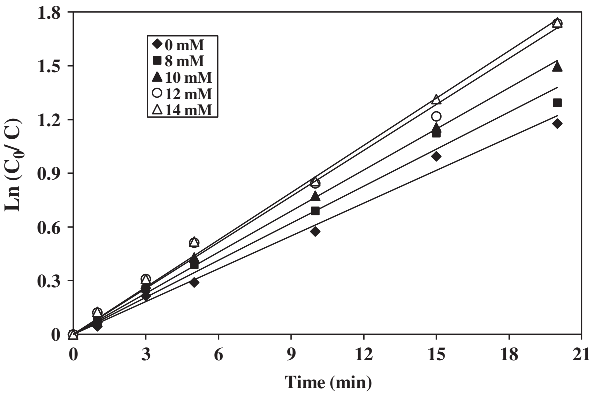

Fig. 6. The change of rate constant as a function of Fe-HPA loading for phenol photodegradation. Experimental conditions: $[C_0] = 1.06$ mM, pH = 2, and $T = 25$°C.

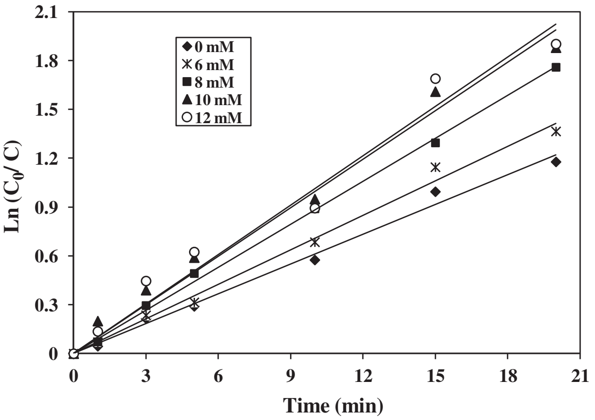

Fig. 7. The change of rate constant as a function of V-HPA loading for phenol photodegradation. Experimental conditions: $[C_0] = 1.06$ mM, pH = 2, and $T = 25$°C.

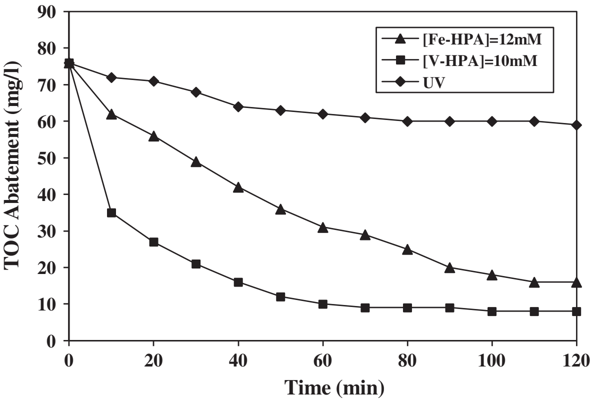

Fig. 8. Temporal changes in total organic carbon (TOC) during different photodegradation processes. Experimental conditions: $[C_0] = 1.06$ mM, TOC = 76 mg/L, $t = 120$ min, pH = 2, and $T = 25$°C.

the V-HPA catalyst has the best catalytic activity with low amount.

3.5. Total mineralization of phenol

The extent of phenol mineralization is examined by determination of the removed amount of TOC. The temporal changes of TOC during the photodegradation process of phenol in presence of Fe-HPA and V-HPA are depicted in Fig. 8.

The study of the complete mineralization of phenol has shown that 74 and 87% of TOC has been removed by Fe-HPA/UV process after 90 min and V-HPA/UV process after 60 min, respectively. The UV irradiation of the sample without catalysts shows extremely low TOC abatement.

TOC remains almost constant even when phenol is completely removed from the solution in the presence of HPA catalysts. This does not mean that the HPA catalyst is not efficient for phenol degradation since some intermediates may be produced.

Many works based on the photocatalytic degradation of phenolic compounds, have thoroughly investigated the mechanism and pathway of phenol mineralization [43–48].

The phenol degradation proceeds primarily by the attack of the hydroxyl radicals, which result in the hydroxylation of the parent compound of phenol. The photocatalytic degradation of phenol yields catechol and/or hydroquinone as the primary hydroxylated intermediates, which on further exposure results on the formation of a fully hydroxylated secondary intermediate species (par-quinone or hydroxyl hydroquinone). This step is followed by the fragmentation of the dihydroxy phenols to form hydroxyl-substituted miconic acid and muconic aldehyde. The latter degrades to simplest organic acids like oxalic acid, maleic acid, fumaric acid, etc. which are further mineralized to form CO_2 and H_2O [45]. Fig. 9 shows the different steps of phenol degradation.

The intermediates formed in AOPs are sometimes more toxic than the parent compounds and are required to be decomposed completely using either combination of AOPs or combination of AOP and some other treatment methods such as adsorption and biodegradation.

3.6. Discussion

Interestingly, the HPA is keeping its structure intact even if it undergoes stepwise multielectron

Table 3
Photolytic reaction constants of HPAs catalysts and correlation coefficient R^2

Fe-HPA (mM)	k (min^{-1})	R^2	V-HPA (mM)	k (min^{-1})	R^2
0	0.0610	0.9916	0	0.0610	0.9916
8	0.0690	0.9873	6	0.0707	0.9930
10	0.0760	0.9965	8	0.0881	0.9982
12	0.0856	0.9931	10	0.0994	0.9820
14	0.0879	0.9957	12	0.1012	0.9711

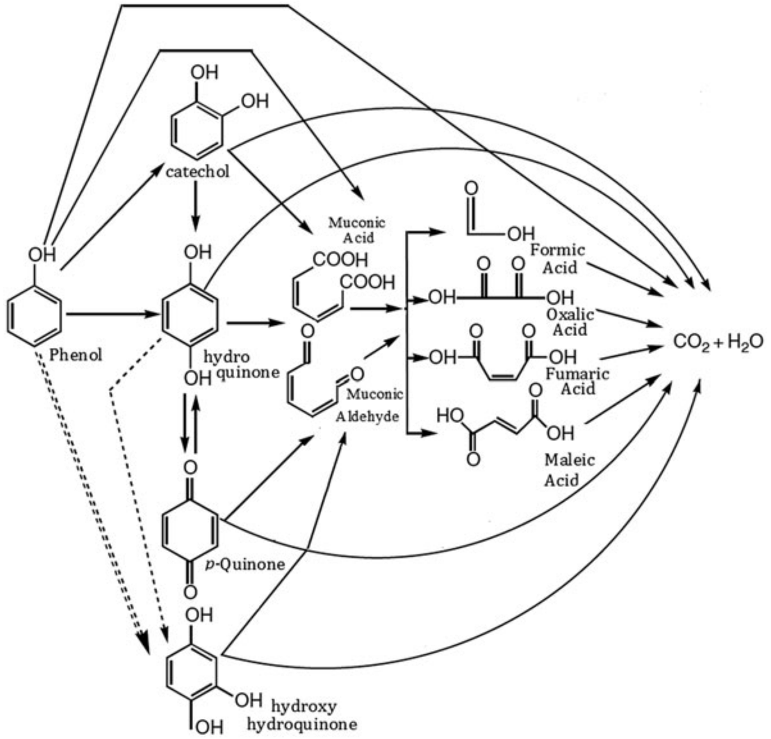

Fig. 9. Detailed pathway of phenol degradation adapted from different studies [45–47].

redox reactions. Thus, HPA can serve as multielectron relays. HPA can also serve as oxygen relays and replenishing the consumed oxygen with atmospheric oxygen. These properties make HPA attractive for applications in photocatalytic degradation.

The proposed mechanistic scheme involving the photocatalytic degradation of phenol in the presence of HPA can be summarized by the photocatalytic cycle in Fig. 10.

Fig. 10 shows the common photocatalytic cycle of HPA, which is similar to the well-known mechanism of semiconductor photocatalysis.

This photocatalytic cycle is explained by proposed mechanisms where the oxidation is supposed to be performed indirectly by highly oxidizing radical $OH^\bullet$ or directly in the presence of the excited HPA $(e^- + h^+)$.

Firstly, in analogy with metal oxide particulates, the excitation of HPA can be considered as electron hole (*h*+) separation, represented as follows:

$$\mathrm{HPA} \overset{hv}{\leftrightarrow} \mathrm{HPA}(e^- + h^+) \tag{8}$$

The electron reduction of HPA upon illumination in the UV area by an electron donor (substrate S) to form the reduced $\mathrm{HPA}(e^-)$ is followed by the easy re-oxidation to its original electron state by an electron acceptor. The substrate reacts directly with the excited HPA (Eq. (9)) or, indirectly via $OH^\bullet$ radicals (Eq. (11)). The latter is generated by the high oxidizing ability of the excited HPA (Eq. (10)).

$$\mathrm{HPA}(e^- + h^+) + \mathrm{S} + \mathrm{Oxidant} \rightarrow \mathrm{S_{Ox}} + \mathrm{HPA}(e^-) \tag{9}$$

$$\mathrm{HPA}(e^- + h^+) + \mathrm{H_2O} \rightarrow \mathrm{HPA}(e^-) + \mathrm{OH}^\bullet + \mathrm{H}^+ \tag{10}$$

$$\mathrm{S} + \mathrm{OH}^\bullet + \mathrm{H} \rightarrow \mathrm{S_{Ox}} + \mathrm{H_2O} \tag{11}$$

where S: substrate (phenol); $\mathrm{S_{Ox}}$: are the oxidation products; and Oxidant: dioxygen is the most common and benign oxidant.

The oxidant restores the reduced $\mathrm{HPA}(e^-)$ to the original oxidized form and undergoes reductive activation by the superoxide radical anion $O_2^{\bullet -}$ (Eq. (12)) where $O_2^{\bullet -}$ can initiate further oxidations (Eq. (13)).

$$\mathrm{HPA}(e^-) + \mathrm{O_2} + \mathrm{H}^+ + e^- \rightarrow \mathrm{HPA} + \mathrm{O_2^{\bullet -}} + \mathrm{H_2O} \tag{12}$$

$$\mathrm{O_2^{\bullet -}} + \mathrm{S} \rightarrow \mathrm{S_{Ox}} \tag{13}$$

Consequently, in the presence of phenol and dioxygen, the reduced $\mathrm{HPA}(e^-)$ is re-oxidized in acidic medium (Eq. (14)).

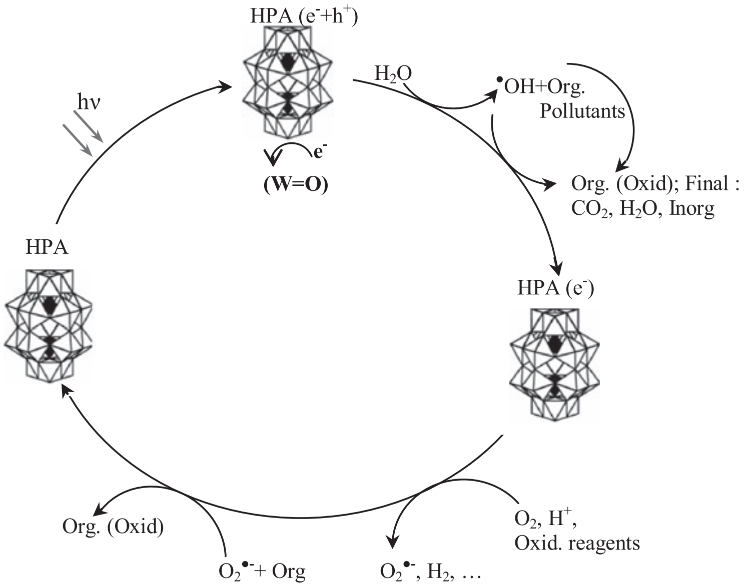

Fig. 10. Schematic diagram of the photocatalytic cycle for Wells–Dawson HPA-mediated photodegradation mechanism.

$$\mathrm{HPA(e^-) + S + O_2 + 4H^+ + 4e^- \rightarrow HPA + S_{Ox} + 2H_2O} \tag{14}$$

Usually, the tungsten HPAs are the catalysts of choice because of their stronger acidity, higher thermal stability, and lower oxidation potential compared to molybdenum HPAs. In addition, the excitation by UV-illumination renders tungstate HPAs powerful oxidizing reagents in relation to molybdate HPAs and their fast re-oxidation by dioxygen makes them the most efficient photocatalysts [49].

Some theoretical and instrumental techniques have been employed to determine the reduction potential of HPAs. According to work of Park et al. [41], the correlations between redox properties and catalytic oxidation activities of $H_4PW_{11}M_1O_{40}$ (M = V, Nb, Ta) and $H_7P_2W_{17}M_1O_{62}$ (M = V, Nb, Ta) catalysts have revealed that their catalytic activity increased with the increasing of reduction potential of the HPA. It has been demonstrated that vanadium-containing HPAs showed excellent redox properties, where the first electron reduction potential of $H_7P_2W_{17}VO_{62}$ catalyst was found to be −0.539 V.

4. Conclusion

In this study, the experimental results demonstrate that the UV technology assisted by HPAs as strong acidic catalysts can be effectively used for degradation of refractory organic compounds such as phenol at a relatively short time $t = 60$ min for $H_7P_2W_{17}VO_{62}.14H_2O$ and $t = 90$ min for $H_5P_2W_{12}Mo_5Fe.10H_2O$.

It is obvious that the photodegradation is strongly influenced by various parameters, particularly pH, irradiation time, and catalysts loading. The photodegradation of phenol is more effective in acidic medium. The optimum pH for the photodegradation is 2 for two HPAs.

The first-order rate expression has been used to describe the photodegradation reaction, where the rate constants $k = 8.56 \times 10^{-2}$ and $9.94 \times 10^{-2}\ \mathrm{min}^{-1}$, respectively, for iron- and vanadium-substituted Dawson HPAs were obtained in the optimal conditions.

The results of TOC indicate that more time is required to complete the mineralization of phenol into water and carbon dioxide by the photocatalysis processes.

The photodegradation study and mineralization test exhibit that the tungstate HPA $H_7P_2W_{17}VO_{62}.14H_2O$ is the most efficient photocatalyst for phenol degradation.

References

[1] Q. Liao, J. Sun, L. Gao, Degradation of phenol by heterogeneous Fenton reaction using multi-walled carbon nanotube supported Fe_2O_3 catalysts, Colloids Surf., A 345 (2009) 95–100.

[2] M. Sathishkumar, A.R. Binupriya, D. Kavitha, R. Selvakumar, R. Jayabalan, J.G. Choi, S.E. Yun, Adsorption potential of maize cob carbon for 2,4-dichlorophenol removal from aqueous solutions: Equilibrium, kinetics and thermodynamics modeling, Chem. Eng. J. 147 (2009) 265–271.

[3] J.R. Domínguez-Vargas, J.A.V. Navarro-Rodríguez, J.B. de Heredia, E.M. Cuerda-Correa, Removal of

chlorophenols in aqueous solution by carbon black low-cost adsorbents. Equilibrium study and influence of operation conditions, J. Hazard. Mater. 169 (2009) 302–308.

[4] S. Ledakowicz, M. Solecka, R. Zylla, Biodegradation, decolourisation and detoxification of textile wastewater enhanced by advanced oxidation processes, J. Biotechnol. 89 (2008) 175–184.

[5] M. Pera-Titus, V. García-Molina, M.A. Baños, J. Giménez, S. Esplugas, Degradation of chlorophenols by means of advanced oxidation processes: A general review, Appl. Catal., B 47 (2004) 219–256.

[6] M. Tekbaş, H.C. Yatmaz, N. Bektaş, Heterogeneous photo-Fenton oxidation of reactive azo dye solutions using iron exchanged zeolite as a catalyst, Microporous Mesoporous Mater. 115 (2008) 594–602.

[7] A. Troupis, E. Gkika, T. Triantis, A. Hiskia, E. Papaconstantinou, Photocatalytic reductive destruction of azo dyes by polyoxometallates: Naphthol blue black, J. Photochem. Photobiol., A 188 (2007) 272–278.

[8] M.T. Pope, Heteropoly and Isopoly Oxometalates in Inorganic Chemistry Concepts, 8, Springer-Verlag, West Berlin, 1983.

[9] L.C.W. Baker, D.C. Glick, Present general status of understanding of heteropoly electrolytes and tracing of some major highlights in history of their elucidation, Chem. Rev. 98 (1998) 3–49.

[10] P. Kormali, A. Troupis, T. Triantis, A. Hiskia, E. Papaconstantinou, Photocatalysis by polyoxometallates and TiO_2: A comparative study, Catal. Today 124 (2007) 149–155.

[11] B. Dawson, The structure of the 9(18)-heteropoly anion in potassium 9(18)-tungstophosphate, $K_6(P_2W_{18}O_{62}).14H_2O$, Acta Cryst. 6 (1953) 113–126.

[12] J.M. Pigga. State of Counter-cations in Polyoxometalate Solutions (PhD thesis), Lehigh University, Pennsylvania, USA, 2010.

[13] F. Cavani, Heteropolycompound-based catalysts: A blend of acid and oxidizing properties, Catal. Today 41 (1998) 73–86.

[14] R. Kaoua, N. Bennamane, S. Bakhta, S. Benadji, C. Rabia, B. Nedjar-Kolli, Synthesis of substituted 1,4-diazepines and 1,5-benzodiazepines using an efficient heteropolyacid-catalyzed procedure, Molecules 16 (2011) 92–99.

[15] A. Troupis, T.M. Triantis, E. Gkika, A. Hiskia, E. Papaconstantinous, Photocatalytic reductive–oxidative degradation of acid orange 7 by polyoxometalates, Appl. Catal., B 86 (2009) 98–107.

[16] T. Yamase, Photo- and electrochromism of polyoxometalates and related materials, Chem. Rev. 98 (1998) 307–326.

[17] I.K. Song, M.A. Barteau, Redox properties of keggin-type heteropolyacid (HPA) catalysts: Effect of counter-cation, heteroatom and polyatom substitution, J. Mol. Catal., A 212 (2004) 229–236.

[18] A. Hiskia, M. Ecke, A. Troupis, A. Kokorakis, H. Hennig, E. Papaconstantinou, Sonolytic, photolytic, and photocatalytic decomposition of atrazine in the presence of polyoxometalates, Environ. Sci. Technol. 35 (2001) 2358–2364.

[19] E. Bae, J.W. Lee, B.H. Hwang, Ji. Yeo, J. Yoon, H.J. Cha, W. Choi, Photocatalytic bacterial inactivation by polyoxometalates, Chemosphere 72 (2008) 174–181.

[20] S. Kim, H. Park, W. Choi, Comparative study of homogeneous and heterogeneous photocatalytic redox reactions: $PW_{12}O^{3-}{}_{40}$ vs. TiO_2, J. Phys. Chem., B 108 (2004) 6402–6411.

[21] I.V. Kozhevnikov, Heteropoly acids and related compounds as catalysts for fine chemical synthesis, Catal. Rev. Sci. Eng. 37 (1995) 311–352.

[22] B. Baghernejad, M.M. Heravi, H.A. Oskooie, F.F. Bamoharram, Heteropolyacids as an efficient and reusable catalytic system for the regiospecific nitration of phenols with metal nitrates, Bull. Chem. Soc. Ethiop. 26 (2012) 145–152.

[23] L.E. Briand, G.T. Baronelti, H. Thomas, The state of the art on Wells–Dawson heteropoly-compounds: A review of their properties and applications, Appl. Catal., A 256 (2003) 37–50.

[24] D.R. Park, H. Kim, J.C. Jung, S.H. Lee, I.K. Song, Correlation between reduction potential of vanadium-containing heteropolyacid (HPA) catalysts and their oxidation activity for cyclohexanol dehydrogenation, React. Kinet. Catal. Lett. 93 (2008) 43–49.

[25] M.T. Pope, A. Müller, Polyoxometalate chemistry: An old field with new dimensions in several disciplines, Angew. Chem. Int. Ed. 30 (1991) 34–48.

[26] M.T. Pope, A. Müller, Polyoxometalates: from Platonic Solids to anti-retroviral activity, Kluwer Academic Publishers, Dordrecht, 1994.

[27] C. Hill (Ed.), Special thematic issue on polyoxometalates, Chem. Rev. 98 (1998) 1–390.

[28] R. Contant, J.P. Ciabrini, Stereospecific preparations of new *n*-molybdo-(18-*n*)-tungsto-2-phosphates and related "defect" compounds (*n* = 2, 4 or 5), J. Inorg. Nucl. Chem. 43 (1981) 1525–1528.

[29] M.T. Pope, G.M. Varga, Heteropoly blues. I. Reduction stoichiometries and reduction potentials of some 12-tungstates, Inorg. Chem. 5 (1966) 1249–1254.

[30] R. Contant, W.G. Klemperer, O. Yaghi, Potassium octadecatungstodiphosphates (V) and related lacunary compounds, Inorg. Synth. 27 (2007) 104–111.

[31] R. Contant, M. Abbessi, J. Canny, M. Richet, A. Belhouari, B. Keita, L. Nadjo, Synthesis, characterization and electrochemistry of complexes complexes derived from $[(1),2,3\text{-}P_2Mo_2W_{15}O_{61}]^{10-}$ and first transition metal ions, Eur. J. Inorg. Chem. 2000 (2000) 567–574.

[32] A. Belhouari, B. Keita, L. Nadjo, R. Contant, Efficient conversion of NO into N_2O by electroreduced selected heteropolyanions, New J. Chem. 22 (1998) 83–86.

[33] M. Abbessi, R. Contant, R. Thouvenot, G. Herve, Dawson type heteropolyanions. 1. Multinuclear (phosphorus-31, vanadium-51, tungsten-183) NMR structural investigations of octadeca(molybdotungstovanado) diphosphates.alpha.-1,2,3-$[P_2MM'_2W_{15}O_{62}]$n- (M, M′ = Mo, V, W): Syntheses of new related compounds, Inorg. Chem. 30 (1991) 1695–1702.

[34] D.K. Lyon, W.K. Miller, T. Novet, P.J. Domaille, E. Evitt, D.V.C. Jonson, R.G. Finke, Highly oxidation resistant inorganic-porphyrin analog polyoxometalate oxidation catalysts. 1. The synthesis and characterization of aqueous-soluble potassium salts of.alpha.2-$P_2W_{17}O_{61}(Mn^+$.cntdot.OH2)(n-10) and organic solvent soluble tetra-n-butylammonium salts of.alpha.2-$P_2W_{17}O_{61}(Mn^+$.cntdot.Br)(n-11) (M = Mn^{3+}, Fe^{3+}, Co^{2+}, Ni^{2+}, Cu^{2+}), J. Am. Chem. Soc. 113 (1991) 7209–7221.

[35] A.V. Petukhov, Effect of molecular mobility on kinetics of an electrochemical Langmuir–Hinshelwood reaction, Chem. Phys. Lett. 277 (1997) 539–544.

[36] C.H. Chiou, C.Y. Wu, R.S. Juang, Influence of operating parameters on photocatalytic degradation of phenol in UV/TiO_2-process, Chem. Eng. J. 139 (2008) 322–329.

[37] N.G. Asenjo, R. Santamaría, C. Blanco, M. Granda, P. Álvarez, R. Menéndez, Correct use of the Langmuir–Hinshelwood equation for proving the absence of a synergy effect in the photocatalytic degradation of phenol on a suspended mixture of titania and activated carbon, Carbon 55 (2013) 62–69.

[38] P. Chin, Kinetics of Photocatalytic Degradation Using Titanium Dioxide Films (PhD thesis), North Carolina State University, USA, 2008.

[39] D. Li, T. Yuranova, P. Albers, J. Kiwi, Accelerated photobleaching of orange II on novel ($H_5FeW_{12}O_{40}.10H_2O$)/silica structured fabrics, Water Res. 38 (2004) 3541–3550.

[40] M.A. Schwegler, Heteropolyacids Catalysts in Organic Reactions (PhD thesis), Delft University of Technology, Netherland, 1991.

[41] D.R. Park, S. Park, Y. Bang, I.K. Song, Redox properties and oxidation catalysis of group 5 metal (V, Nb, Ta)-containing Keggin and Wells–Dawson heteropolyacid (HPA) catalysts, Appl. Catal., A 373 (2010) 201–207.

[42] I.V. Kozhevnikov, Catalysis by heteropolyacids and multicomponent polyoxometalates in liquid-phase reactions, Chem. Rev. 98 (1998) 171–198.

[43] E.F. Mohamed, Removal of Organic Compounds from Water by Adsorption and Photocatalytic Oxidation (PhD thesis), National Polytechnic Institute of Toulouse, France, 2011.

[44] L. Zhangi, T. Kanki, N. Sano, A. Toyoda, Pathways and kinetics on photocatalytic destruction of aqueous phenol, Environ. Monit. Assess. 115 (2006) 395–403.

[45] R. Vinu, G. Madras, Environmental remediation by photocatalysis, J. Indian Inst. Sci. 90 (2010) 189–230.

[46] A. Ortiz-Gomez, Enhanced Mineralization of Phenol and other Hydroxylated Compounds in a Photocatalytic Process assisted with Ferric Ions (PhD thesis), The University of Western Ontario, Canada, 2006.

[47] A. Ortiz-Gomez, B. Serrano-Rosales, H. de Lasa, Enhanced mineralization of phenol and other hydroxylated compounds in a photocatalytic process assisted with ferric ions, Chem. Eng. Sci. 63 (2008) 520–557.

[48] J. Moreira del Rio, Photocatalytic Degradation of Phenolic Compounds in Water: Irradiation and Kinetic Modeling (PhD thesis), The University of Western Ontario, Canada, 2011.

[49] R.S. Weber, Molecular orbital study of C–H bond breaking during the oxidative dehydrogenation of methanol catalyzed by metal oxide surfaces, J. Phys. Chem. 98 (1994) 2999–3005.